Lawrence Berkeley Laboratory
UNIVERSITY OF CALIFORNIA

Submitted to Physical Review C

TARGET RESIDUE RECOIL PROPERTIES IN THE INTERACTION OF 8.0 GeV ^{20}Ne WITH ^{181}Ta

W. Loveland, D. J. Morrissey, K. Aleklett, G. T. Seaborg,
S. B. Kaufman, E. P. Steinberg, B. D. Wilkins,
J. B. Cumming, P. E. Haustein, and H. C. Hseuh

May 1980

Prepared for the U.S. Department of Energy under Contract W-7405-ENG-48

DISCLAIMER

TARGET RESIDUE RECOIL PROPERTIES IN THE INTERACTION OF 8.0 GeV ^{20}Ne WITH ^{181}Ta

W. Loveland
Department of Chemistry, Oregon State University, Corvallis, OR 97331

D. J. Morrissey, K. Aleklett* and G. T. Seaborg
Nuclear Science Division, Lawrence Berkeley Laboratory,
University of California, Berkeley, CA 94720

S. B. Kaufman, E. P. Steinberg and B. D. Wilkins
Chemistry Division, Argonne National Laboratory, Argonne, IL 60439

J. B. Cumming, P. E. Haustein, and H. C. Hseuh
Chemistry Department, Brookhaven National Laboratory,
Upton, N. Y. 11973

ABSTRACT

The thick target-thick catcher technique has been applied to determine the average kinematic properties of a number of target-fragmentation products formed in the reaction of 8.0 GeV (400 MeV/amu) ^{20}Ne with ^{181}Ta. The forward momentum transferred to the target as a function of product mass is larger than that for the reaction of 25 GeV ^{12}C or relativistic protons with heavy targets, suggesting that limiting fragmentation has not been achieved in the interaction of 8 GeV ^{20}Ne projectiles with a ^{181}Ta target.

*Permanent Address: Studsvik Scientific Research Laboratory, Nykoping, Sweden.

NUCLEAR REACTIONS: $^{181}Ta(^{20}Ne, spallation)$, E = 8.0 GeV; measured target residue recoil properties; relativistic heavy ion reactions; thick-target, thick-catcher technique; Ge(Li) spectroscopy.

The concept of "limiting fragmentation"[1] or "scaling"[2] has been used widely to describe target fragmentation in relativistic nuclear collisions. This hypothesis states that the distribution of products in the rest frame of the projectile or target approaches a limiting form as the bombarding energy increases or, experimentally that a particular distribution changes negligibly over a large range of bombarding energies. The physical basis of this concept is that, due to Lorentz contraction of the projectile, the projectile-target interaction time at any given impact parameter becomes independent of bombarding energy.

Support for the application of this concept to describe relativistic nuclear collisions comes from the observation of Cumming, et al.[3] that the product mass and charge distributions from the spallation of Cu by 80 GeV ^{40}Ar, 25 GeV ^{12}C and 3.9 GeV ^{14}N were similar and the observation of Loveland et al.[4] that the same situation occurs in the interactions of 8 GeV ^{20}Ne and 25 GeV ^{12}C with ^{181}Ta. In both cases the experimenters observed that the distributions from the relativistic heavy ion reactions were generally similar to the distributions produced in reactions induced by protons of the same total kinetic energy. These latter observations coupled with the observation of Kaufman et al.[5] that the forward momentum transferred to a ^{197}Au target nucleus by 25 GeV ^{12}C ions was essentially identical to that transferred by 28 GeV protons suggested that studies of target fragmentation would not be sensitive indicators of the new aspects of nuclear behavior expected to be seen in relativistic heavy ion reactions or that no new phenomena are occurring. Small deviations from the limiting fragmentation hypothesis

were observed, however, for the recoil properties of fragments from the reaction of 25 GeV ^{12}C with Cu^{6}.

In this paper we describe an interlaboratory study of the product recoil properties from the reaction of 8.0 GeV ^{20}Ne with ^{181}Ta, from which the mean kinetic properties can be derived. We will show that despite the results[4] of the measurement of the product mass and charge distributions cited above, the product kinetic properties are not independent of bombarding energy for the (projectile-target) energy and mass region spanned by the 8 GeV ^{20}Ne + ^{181}Ta and 25 GeV ^{12}C + ^{197}Au reactions and furthermore, that the specific product forward momenta observed in the reaction of 8.0 GeV ^{20}Ne with ^{181}Ta exceed those observed in relativistic proton induced reactions with heavy targets. The good agreement between the independent measurements of the three laboratories demonstrates that these very important kinematic parameters describing relativistic nuclear collisions can be reliably measured.

II. Experimental

A stack of ^{181}Ta metal foils (see Fig. 1) was irradiated for approximately 18 hours (total particle fluence 3.6×10^{13} ^{20}Ne) with an external beam of 8.0 GeV ^{20}Ne ions at the LBL Bevalac. In this foil stack there were three separate target assemblies belonging to the cooperating groups from LBL, ANL and BNL. The LBL targets consisted of three ^{181}Ta foils (of thickness 40.4, 42.5 and 41.6 mg/cm^2) surrounded by forward and backward Mylar catcher foils of thickness 35.5 mg/cm^2. As shown in Fig. 1, the three LBL targets were spatially separated from each

other by a distance of 8 cm. The ANL target stack consisted of four ^{181}Ta foils (total ^{181}Ta thickness 176 mg/cm^2), each surrounded by two Mylar cather foils of thickness 18 mg/cm^2. Guard foils (18 mg/cm^2 Mylar) intervened between each of the four ANL targets and the assembly was vacuum sealed in a Mylar envelope. The BNL target stack consisted of a single ^{181}Ta foil of thickness 92.6 mg/cm^2 surrounded on each side by three 18 mg/cm^2 Mylar foils and vacuum sealed in a Mylar envelope. The target assemblies thus represented a variety of approaches to the problem of target arrangement and comparisons between the results of the different groups were expected to be enlightening concerning the role of reactions induced by secondary particles in these studies. The total beam energy loss in the combined ^{181}Ta-Mylar target assembly was calculated to be ∿230 MeV with a beam attenuation due to nuclear scattering of 4.5%.

Assay of the radioactivities in the LBL targets and catcher foils by X-ray and γ-ray spectroscopy began approximately two hours after end of irradiation. The assay of the BNL and ANL target radioactivities began 30 hours after the end of irradiation with these measurements being delayed by air shipment of the targets to the respective laboratories. In the case of the LBL targets, the three foward catcher foils were placed together and counted as a single sample as were the three backward foils. One representative ^{181}Ta foil was counted and a correction for the uncounted targets was made to each nuclide activity. A similar procedure was followed for the ANL targets except that all target foils were placed together and counted as a single high activity sample. Standard techniques which have been described elsewhere[3,7,8] were used

to identify the radionuclides present in each sample and to determine the activity of each nuclide in the forward, backward and target foils. No corrections were made to any of the foil activities for the effect of secondary induced reactions because previous studies[9] had shown that over the range of target thicknesses encountered in this experiment, the effect of secondary reactions was negligible ($\leqslant$4 percent) and our own observation that the measurements of the different laboratories using vastly different target arrangements were the same within experimental uncertainty. The guard foils were used to measure the amount of any products whose range exceeded the thickness of the catcher foils, as well as any activity due to impurities. The only such activity found was that of ^{24}Na from impurity activation; the correction for this effect amounted to $\leqslant$1 percent.

III. Results

The results of these measurements are presented as the fractions of each radionuclide which recoiled out of a target of thickness W(mg/cm^2) in the forward and backward directions denoted by F and B, respectively. Table I gives a tabulation of the combined results of the three groups for the forward-to-backward ratio, F/B and a quantity approximately equal to the mean range of the recoil in the target material, 2W (F+B). The data shown in Table I and plotted in Fig. 2 are the weighted averages of the measurements of the different laboratories which, in general, agreed within experimental uncertainty. Each product recoil property reported in Table I was measured by at least two of the three laboratories. In performing the weighted average

calculation the minmum uncertainty in the results of a single laboratory was arbitrarily assumed to be at least ± 5%, although the measured uncertainty may have been less. This procedure was done to insure that each laboratory's results affected the weighted average in this interlaboratory comparison and because we believe there are systematic uncertainties in this type of measurement of at least 5%.

The results were transformed into kinematic quantities using the two step vector model of high energy nuclear reactions, developed by Sugarman and co-workers.[10-12] The equations used in the analysis have been recently described by Winsberg.[13] In this model, the velocity, $\vec{V}_\ell$, of a recoil nuclide in the laboratory system is taken to be the sum of the two vectors

$$\vec{V}_\ell = \vec{v} + \vec{V}$$

The velocity vector $\vec{v}$ results from the initial fast projectile-target interaction (the "abrasion" step of the abrasion-ablation model[14]) while the velocity vector $\vec{V}$, assumed to be isotropic in the moving system, results from the slow de-excitation of the excited primary fragment (the "ablation step"). The vector $\vec{v}$ is assumed to be constant while the values of the vector $\vec{V}$ are assumed to have a Maxwellian distribution. No correlation is assumed to exist between the two vectors. The vector $\vec{v}$ can be decomposed into its two orthogonal components parallel and perpendicular to the beam ($v_\parallel$ and $v_\perp$) and in this analysis we have assumed $v_\perp = 0$. In converting product ranges into kinetic energies, we used the range-energy tables of Northcliffe and Schilling.[15] For ranges lower that those tabulated (as was the case for ^{171}Lu) a range-proportional-to-energy extrapolation was used. The resulting range-energy curve is in reasonable agreement (±10%) with that predicted by

the stopping power theory of Lindhard, Scharff and Schiott.[16] The results of this analysis are shown in Table II and Fig. 3.

The validity of this analysis depends on the assumptions stated above. The assumption of the isotropy of $\vec{V}$ in the moving system implies that the observed forward peaking seen in the values of F/B arises from the forward component of $\vec{v}$, namely $\vec{v}_{\|}$. Anisotropies of $\vec{V}$ have been observed[17] for light nuclear fragments in proton-induced reactions at GeV energies, and there may be even larger anisotropies present in relativistic heavy-ion reactions. The investigation of these effects requires measurements of the differential cross sections, $d^2\sigma/d\Omega dE$, which have not yet been made, owing to the low beam intensities available. In spite of these uncertainties, however, comparisons between different projectiles and energies can be informative and can guide the course of future investigations.

IV. Discussion of Results

Some general features of the data are immediately apparent from looking at Fig. 2. The F/B values represent the extent of forward-peaking of the recoils and thus are a combined measure of the recoil angular distribution and the recoil ranges. As seen in Fig. 2, there is a rapid increase in forward-peaking with increasing mass loss from the target (decreasing A) until about 40 nucleons have been lost. With further mass loss the F/B values decrease until one reaches the lightest products ($A<50$) whereupon the F/B values increase with decreasing fragment A.

This general variation of F/B values with product mass is similar to that observed in the interaction of relativistic protons ($1 \leqslant Ep \leqslant 300$ GeV) with ^{197}Au[7] and the interaction of 450 and 580 MeV protons with ^{181}Ta.[11,18] The large values of F/B near A 145-150 were not seen in the interaction of 19 GeV protons with ^{181}Ta.[18] However, a detailed comparison of the F/B values measured in this work for the reaction of 8.0 GeV ^{20}Ne with ^{181}Ta with similar values from the reaction of 580 MeV protons with ^{181}Ta[18] or 3-11.5 GeV protons with ^{197}Au[7] or 25 GeV ^{12}C ions with ^{197}Au[5] or ^{181}Ta[4] (see Fig. 4) reveals that while the trend of F/B with product mass A is similar for all systems, the product F/B values for the 8.0 GeV ^{20}Ne + ^{181}Ta reaction exceed any equivalent values for the other reactions. (This conclusion is independent of whether one compares F/B values for products of the same A for the ^{181}Ta target and ^{197}Au target reactions or whether one compares products with the same ΔA removed from the target).

From these F/B values (and the forward velocity or angular distributions they represent) we can conclude that limiting fragmentation (with respect to kinetic properties) has not been attained in the interaction of 8 GeV ^{20}Ne with ^{181}Ta. This conclusion is based upon the non-equivalence of the F/B value for the reaction of 8 GeV ^{20}Ne with ^{181}Ta (this work), 25 GeV ^{12}C with ^{181}Ta[4] and 25 GeV ^{12}C with ^{197}Au.[5] This idea is further supported by the failure[9] of the abrasion-ablation model to describe the product mass and charge distributions in the reaction of 8.0 GeV ^{20}Ne with ^{181}Ta. This model, which is based upon the assumption of limiting fragmentation, has been successfully applied[19] to describe the product mass and charge distributions

in the reaction of 25.2 GeV ^{12}C ions with a wide range of nuclei. This inapplicability of limiting fragmentation (with respect to kinetic properties) appears to be nominally at variance with the work of Cumming et al.[3] who found the product mass yield curves to be very similar for the interaction of 3.9 GeV ^{14}N and 25.2 GeV ^{12}C with copper (e.g., limiting fragmentation with respect to product yields). We feel that we can understand this difference in terms of the fact that the mass yield curves are not sensitive indicators of some details of the reaction mechanism (see discussion below). This raises the question of when the onset of limiting fragmentation takes place. A reasonable criterion might be that this might occur when the projectile velocity, V_p, is 0.9c, i.e., 20 GeV ^{20}Ne, based upon the idea that further increases in the projectile velocity could only change the interaction time by 10%. At 8.0 GeV, ^{20}Ne, $V_p = 0.71c$ and limiting fragmentation might not be expected.

The insensitivity of product mass yield curves to some important details of the reaction mechanism as indicated by the comparison of the results of this work and those by Cumming et al. is given further confirmation by examining the results of Loveland et al.[4] who found with the exception of products with $A < 50$, the product mass distributions, from the reaction of 25.2 GeV ^{12}C, 8.0 GeV ^{20}Ne and 5.7 GeV p with ^{181}Ta were very similar (see Fig. 5). This insensitivity of the product mass distributions to details of the reaction mechanism can be understood in terms of the calculations of Morrissey et al.[20] who showed that for ^{40}Ar projectile fragments that were more than $\sim$1 charge unit away from the projectile, the product mass and charge

distributions were not sensitive to the primary product distribution after the fast step of the reaction but rather were governed by the shape of the valley of β-stability and other parameters related to the statistical deexcitation of the products.

It is instructive to compare the momenta imparted to selected target fragments in the ablation phase (or second step) of the reaction since variation of this property with changes of projectile type and energy can reveal the extent to which the ablation phase of the reaction mechanism is influenced by the abrasion process which occurs during the initial projectile-target interaction. Figure 6 shows a plot of $\langle P \rangle = A \langle V \rangle$ versus A for the spallation of Ta by 8.0 GeV ^{20}Ne and by protons of 0.45,[11] 0.58,[18] and 19 GeV.[18]

For the 8.0 GeV ^{20}Ne induced reaction a steady increase in $\langle P \rangle$ is observed as one moves from near-target products to those that have resulted from the removal of ∿50 nucleons from ^{181}Ta. This increase in $\langle P \rangle$ goes approximately as $\sqrt{\Delta A}$, and is indicative of sequential, step-wise momentum "kicks" being imparted, in a random walk fashion, to the ablating target fragment. A semiempirical theory for such processes developed for proton induced reactions[27] predicts that $\langle P \rangle$ should vary from 15.2 $(\text{MeV}\cdot A)^{1/2}$ for ^{171}Lu to 34.5 $(\text{MeV}\cdot A)^{1/2}$ for ^{131}Ba in agreement with the trend of the present results. Neidhart and Bächmann[18] have reported no energy dependence of $\langle P \rangle$ for rare earth nuclides formed by irradiation of Ta with 0.58 and 19 GeV protons. Their mean values shown in Fig. 6 fall somewhat below our for products with A < 165 but agree for ^{167}Tm and ^{171}Lu. The general pattern based on these results for Ta and those for Au

targets[5,8] is that the ablation phase of reactions leading to products with $\Delta A \lesssim 50$ is essentially energy and projectile invariant.

Below A=100 the target fragments from the 8.0 GeV ^{20}Ne induced spallation of Ta exhibit a saturation in <P> at $\sim$50 (MeV·amu)$^{1/2}$. For comparison with the present results, values of <P> obtained by Porile and Sugarman[11] for neutron-rich products such as ^{91}Sr from the interaction of 0.45 GeV protons with Ta have been included in Fig. 6. These exhibit a parabolic dependence of <P> on A centered at A $\approx$ 81, consistent with a binary fission mechanism. In a narrow mass region near the peak of the parabola, Trabitzsch and Bächmann[18] have studied products spanning a wide range of neutron to proton ratios for 0.58 and 19 GeV protons. Their values of <P> shown in Fig. 6 appear to scatter over a considerable range at either energy. As was pointed out by those authors and can be seen in Fig. 7, this reflects a significant dependence of <P> on N/A. Results for 8 GeV ^{20}Ne projectiles fall between, but closer to the higher energy proton values. Based on the more extensive data for Au targets,[8] the Ne + Ta values approximate those expected if proejectile kinetic energy was the important scaling variable. They are obviously different from those of protons having the same velocity as the ^{20}Ne. The low values of <P> for both ^{20}Ne ions and 19 GeV protons and the shape of the mass yield curves (Fig. 5) suggests that fission is not a dominant contributor to middle mass products in either case.

In summary of the experimental data, we can say that we have found that in the reaction of 8.0 GeV ^{20}Ne with ^{181}Ta, a greater fraction of the products recoil forward than in the reaction of equivalent

total energy protons or 25 GeV ^{12}C ions with heavy targets but the de-excitation of the fragments following the initial fast step of the reaction proceeds in a similar manner with modest differences between projectile-target systems. The greater F/B ratios in the 8.0 GeV ^{20}Ne + ^{181}Ta reaction compared to the reaction of 25 GeV ^{12}C with either ^{181}Ta or ^{197}Au may be akin to the decrease in F/B in proton-induced reactions from 3 to 11.5 GeV. For proton induced reactions, this decrease is generally associated[21-24] with a shift in the product angular distribution from forward-peaking to sideward-peaking. While the mechanism for the sidewise peaking is not established (although interesting arguments concerning nuclear shock waves,[22,25] low energy transverse hadron fluxes[21] and a fast two body breakup mechanism[26] have been advanced), it may be that studies of relativistic heavy ion reactions will furnish important insights into the details of the mechanism(s) involved. It thus appears that significant opportunities for studying new and exciting aspects of nuclear interactions exist in the study of target fragmentation in relativistic heavy ion reactions and furthermore, that the study of the product angular distributions and momenta hold the greater promise for increasing our understanding of these processes.

Financial support for this work was provided in part by the U.S. Department of Energy under Contract W-7405-ENG-48.

Table I

Target Fragment Recoil Properties for 8.0 GeV ^{20}Ne + Ta.

Nuclide	E (keV)	LBL		ANL		BNL		Wtd. Average	
		F/B	2W(F+B)	F/B	2W(F+B)	F/B	2W(F+B)	F/B	2W(F+B)
^{24}Na	1368.6, 2753.9	5.9 ± 0.4	17.1 ± 1.7	5.44 ± 0.30	15.8 ± 1.0	5.90 ± 0.13	17.42 ± 0.33	5.72 ± 0.19	16.77 ± 0.61
^{28}Mg	1777.8	5.2 ± 0.8	13.7 ± 1.4	4.71 ± 0.35	15 ± 1.6	4.64 ± 0.23	13.71 ± 0.88	4.69 ± 0.19	13.9 ± 0.68
^{43}K	617.8	3.4 ± 0.7	9.8 ± 2.0	3.4 ± 0.5	7.1 ± 1.0	--------		3.40 ± 0.41	7.64 ± 0.89
^{46}Sc	889.3, 1120.5	------		3.07 ± 0.2	6.9 ± 0.8	3.09 ± 0.09	6.94 ± 0.48	3.08 ± 0.12	6.93 ± 0.32
^{48}Sc	1037.5, 1312.1	3.1 ± 0.6	6.2 ± 0.9	3.11 ± 0.25	7.2 ± 0.9	3.11 ± 0.17	7.91 ± 0.26	3.11 ± 0.14	7.57 ± 0.34
^{48}V	983.5, 1312.1	------		3.06 ± 0.25	7.4 ± 0.5	3.02 ± 0.20	7.64 ± 0.16	3.04 ± 0.16	7.55 ± 0.30
^{54}Mn	834.8	------		2.97 ± 0.30	6.9 ± 0.8	2.61 ± 0.27	7.22 ± 0.34	2.77 ± 0.20	7.17 ± 0.33
^{65}Zn	1115.5	------		2.8 ± 0.7	5.9 ± 0.9	2.27 ± 0.39	6.49 ± 0.66	2.40 ± 0.34	6.28 ± 0.53
^{74}As	595.6	3.3 ± 0.8	4.7 ± 0.9	2.77 ± 0.25	5.7 ± 0.6	2.54 ± 0.20	5.25 ± 0.18	2.65 ± 0.15	5.28 ± 0.23
^{75}Se	264.6	------		3.3 ± 0.5	4.7 ± 0.6	2.45 ± 0.29	4.68 ± 0.26	2.66 ± 0.25	4.68 ± 0.24
^{83}Rb	529.5, 552.7	------		3.95 ± 0.6	4.0 ± 0.5	3.49 ± 0.36	4.79 ± 0.37	3.61 ± 0.31	4.51 ± 0.30
^{84}Rb	881.5	------		3.1 ± 0.3	5.3 ± 0.7	2.70 ± 0.30	5.42 ± 0.29	2.90 ± 0.21	5.4 ± 0.27
^{87}Y	388.3, 484.8	4.7 ± 0.5	3.9 ± 0.4	3.8 ± 0.4	5.0 ± 0.6	4.28 ± 0.09	4.28 ± 0.07	4.27 ± 0.16	4.17 ± 0.16
^{89}Zr	909.2	2.2 ± 0.2	3.1 ± 0.5	4.2 ± 0.4	4.3 ± 0.4	4.58 ± 0.12	4.40 ± 0.08	4.50 ± 0.20	4.38 ± 0.19
^{90}Nb	1129.2	4.3 ± 0.9	3.6 ± 0.7	4.9 ± 0.6	4.3 ± 0.5	6.3 ± 1.3	3.94 ± 0.34	4.92 ± 0.47	3.99 ± 0.26
^{96}Tc	778.2, 849.9	3.6 ± 1.1	4.3 ± 0.9	4.8 ± 0.7	4.1 ± 0.8	4.96 ± 0.43	4.31 ± 0.17	4.78 ± 0.35	4.30 ± 0.21
^{97}Ru	215.7	5.0 ± 1.5	4.7 ± 0.5	7.8 ± 0.8	3.0 ± 0.6	--------		7.18 ± 0.71	4.00 ± 0.38
^{131}Ba	496.2	-----	2.5 ± 0.4	16 ± 3	2.0 ± 0.25	13.5 ± 1.0	2.30 ± 0.03	13.75 ± 0.95	2.26 ± 0.10
^{139}Ce	165.8	------		15 ± 4	1.9 ± 0.2	17.8 ± 6.4	1.95 ± 0.04	15.79 ± 3.39	1.94 ± 0.09
^{145}Eu	893.7	-----	1.4 ± 0.2	20 ± 3	1.35 ± 0.12	16.9 ± 3.5	1.59 ± 0.06	18.69 ± 2.28	1.50 ± 0.06
^{146}Gd	115.5, 747.1	------		19 ± 3	1.37 ± 0.20	13.3 ± 2.5	1.58 ± 0.03	15.64 ± 1.92	1.55 ± 0.07
^{149}Gd	149.7	25 ± 15	1.0 ± 0.1	23 ± 4	1.31 ± 0.15	16.5 ± 1.9	1.36 ± 0.02	17.70 ± 1.72	1.26 ± 0.05
^{167}Tm	207.8	-----	0.2 ± 0.05	11 ± 3	0.39 ± 0.06	11.3 ± 2.1	0.42 ± 0.03	11.20 ± 1.72	0.37 ± 0.02
^{171}Lu	739.6	-----	0.08 ± 0.04	8.6 ± 2.5	0.22 ± 0.04	10.0 ± 1.7	0.23 ± 0.01	9.56 ± 1.41	0.22 ± 0.01

Table II

Target fragment kinematic properties as deduced from the Two Step Vector Model.

Nuclide	k^*	N^*	R (mg/cm^2)	v $(MeV/amu)^{1/2}$	$\beta_{\parallel}$ (= v /c)	V $(MeV/amu)^{1/2}$	< E > (MeV)
^{24}Na	0.543	1.71	13.9	0.651	0.0213	1.80	44.2
^{28}Mg	0.564	1.66	11.9	0.516	0.0169	1.64	42.5
^{43}K	1.135	1.15	6.87	0.300	0.00982	1.02	25.4
^{46}Sc	1.173	1.10	6.34	0.262	0.00860	0.960	24.0
^{48}Sc	1.195	1.10	6.90	0.275	0.00900	0.998	27.0
^{48}V	1.129	1.09	6.90	0.290	0.00950	1.068	31.0
^{54}Mn	1.140	1.08	6.65	0.243	0.00798	0.979	29.3
^{65}Zn	1.086	1.08	5.95	0.181	0.00592	0.842	26.1
^{74}As	0.957	1.15	4.92	0.160	0.00524	0.676	19.1
^{75}Se	0.866	1.20	4.36	0.145	0.00475	0.620	16.3
^{83}Rb	0.866	1.19	4.01	0.170	0.00557	0.555	14.5
^{84}Rb	0.871	1.19	4.97	0.168	0.00550	0.656	20.6
^{87}Y	0.724	1.30	3.60	0.172	0.00563	0.510	12.8
^{89}Zr	0.711	1.311	3.76	0.149	0.00489	0.524	13.9
^{90}Nb	0.691	1.31	3.33	0.180	0.00590	0.486	12.0
^{96}Tc	0.666	1.33	3.60	0.183	0.00600	0.503	13.7
^{97}Ru	0.613	1.38	3.05	0.204	0.00667	0.448	11.0
^{131}Ba	0.322	1.76	1.44	0.154	0.00505	0.276	5.64
^{139}Ce	0.284	1.86	1.19	0.142	0.00466	0.245	4.74
^{145}Eu	0.235	1.95	0.871	0.131	0.00430	0.217	3.87
^{146}Gd	0.228	1.96	0.947	0.130	0.00425	0.229	4.31
^{149}Gd	0.228	1.96	0.649	0.111	0.00362	0.187	2.94
^{167}Tm	0.227	1.97	0.248	0.054	0.00177	0.108	1.10
^{171}Lu	0.197	2.00	0.153	0.0422	0.00138	0.090	0.78

*The range of the fragments, R, in the target material, Ta, is assumed to be given as $R = kE^{N/2}$ where E is the kinetic energy of the fragment in the system moving with velocity $v_{\parallel}$.

References

1. J. Benecke, T. T. Chou, C. N. Yang, and E. Yen, Phys. Rev. 188, 2159 (1969).

2. R. P. Feynman, Phys. Rev. Lett. 23, 1415 (1969).

3. J. B. Cumming, R. W. Stoenner, and P. E. Haustein, Phys. Rev. C14, 1554 (1976); J. B. Cumming, P. E. Haustein, R. W. Stoenner, L. Mausner and R. A. Naumann, Phys. Rev. C10, 739 (1974); J. B. Cumming, P. E. Haustein, T. J. Ruth, and G. J. Virtes, Phys. Rev. C17, 1632 (1978).

4. W. Loveland, D. J. Morrissey and G. T. Seaborg, Oregon State University Report RLO-2227-TA35-1; D. J. Morrissey, W. Loveland and G. T. Seaborg, Z. Physik A289, 123 (1978).

5. S. B. Kaufman, E. P. Steinberg and B. D. Wilkins, Phys. Rev. Lett. 41, 1359 (1978).

6. J. B. Cumming, P. E. Haustein and H. C. Hseuh, Phys. Rev. C18, 1372 (1978).

7. D. J. Morrissey, D. Lee, R. J. Otto, and G. T. Seaborg, Nucl. Instr. Meth. 158, 499 (1978).

8. S. B. Kaufman, E. P. Steinberg and M. W. Weisfield, Phys. Rev. C18, 1349 (1978).

9. D. J. Morrissey, W. Loveland, M. De Saint-Simon, and G. T. Seaborg, Phys. Rev. C (accepted for publication).

10. N. Sugarman, M. Campos and K. Wielgoz, Phys. Rev. 101, 388 (1956).

11. N. T. Porile and N. Sugarman, Phys. Rev. 107, 1410 (1957).

12. N. Sugarman, H. Munzel, J. A. Panontin, K. Wielgoz, M. V. Ramaniah, G. Lange, and E. Lopez-Menchero, Phys. Rev. 143, 952 (1966).

13. L. Winsberg, Nucl. Instr. Meth. 150, 465 (1978).

14. J. D. Bowman, W. J. Swiatecki and C. F. Tsang, Lawrence Berkeley Laboratory Report No. LBL-2908, 1973 (unpublished); see also J. Gossett, H. H. Gutbrod, W. G. Meyer, A. M. Poskanzer, A. Sandoval, R. Stock, and G. D. Westfall, Phys. Rev. C16, 629 (1977).

15. L. C. Northcliffe and R. F. Schilling, Nucl. Data A7, 233 (1970).

16. J. Lindhard, M. Scharff and H. E. Schiott, Kgl. Danske Videnskab. Sellskab., Mat-Fys. Medd. 33, 14 (1963).

17. J. B. Cumming, R. J. Cross, J. Hudis, and A. M. Poskanzer, Phys. Rev. 134, B167 (1964); A. M. Poskanzer, G. Butler and E. K. Hyde, Phys. Rev. C3, 882 (1971); G. D. Westfall, R. Sextro, A. M. Poskanzer, A. Zebelman, G. Butler, and E. K. Hyde, Phys. Rev. C17, 1368 (1978).

18. B. Neidhart and K. Bachmann, J. Inorg. Nucl. Chem. 34, 423 (1972); U. Trabitzsch and K. Bachmann, Radiochemica Acta, 16, 129 (1974).

19. D. J. Morrissey, W. R. Marsh, R. J. Otto, W. Loveland, and G. T. Seaborg, Phys. Rev. C18, 1267 (1978).

20. D. J. Morrissey, L. F. Oliveira, J. O. Rasmussen, G. T. Seaborg, Y. Yariv, and Z. Fraenkel, Phys. Rev. Lett. 43, 1179 (1979).

21. D. R. Fortney and N. T. Porile, Phys Lett. 76B, 553 (1978).

22. L. P. Remsberg and D. G. Perry, Phys. Rev. Lett. 35, 361 (1975).

23. N. T. Porile, S. Pandian, H. Klonk, C. R. Rudy and E. P. Steinberg, Phys. Rev. C19, 1832 (1979).

24. N. T. Porile, D. R. Fortney, S. Pandian, R. A. Johns, T. Kaiser, K. Wielgoz, T. S. K. Chang, N. Sugarman, J. A. Urbon, D. J. Henderson, S. B. Kaufman, and E. P. Steinberg, Phys. Rev. Lett. 43, 918 (1979).

25. A. E. Glassgold, W. Heckrotte and K. M. Watson, Ann. Phys. (New York) 6, 1 (1959).

26. B. D. Wilkins, S. B. Kaufman, E. P. Steinberg, J. A. Urbon, and D. J. Henderson, Phys. Rev. Lett. 43, 1080 (1979).

27. V. P. Crespo, J. B. Cumming, and J. M. Alexander, Phys. Rev. C 2, 1777 (1970).

Figure Captions

Figure 1. Schematic diagram of target foil array.

Figure 2. Target fragment recoil properties from the interaction of 8 GeV ^{20}Ne with ^{181}Ta.

Figure 3. Target fragment kinetic properties deduced from recoil data using the two-step vector model for the reaction of 8.0 GeV ^{20}Ne with ^{181}Ta.

Figure 4. Comparison of target fragment F/B ratios for various relativistic proton and heavy ion reactions with ^{181}Ta and ^{197}Au.

Figure 5. Target fragment mass distributions for the interaction of 5.7 GeV protons, 8.0 GeV ^{20}Ne and 25 GeV ^{12}C with Ta.

Figure 6. Dependence of fragment momentum on product mass for the interaction of ^{20}Ne ions and protons with Ta. Data points are for: 8 GeV ^{20}Ne, ●, the present work; 0.45 GeV ^{1}H, ○, ref. 11; 0.58 GeV ^{1}H, ■, ref. 18; and 19 GeV ^{1}H, □, also ref. 18. The solid curve through the filled circles for $A > 130$ is given by $P = 5.15\sqrt{\Delta A}$ where $\Delta A = 181 = A$. The upper most curve is a parabola through the open circles. The remaining curves serve to guide the eye through the present data.

Figure 7. Dependence of fragment momentum on product neutron/proton ratio. Data are from the present work (●) and ref. 18 (□ and ■). The lines incidate general trends.

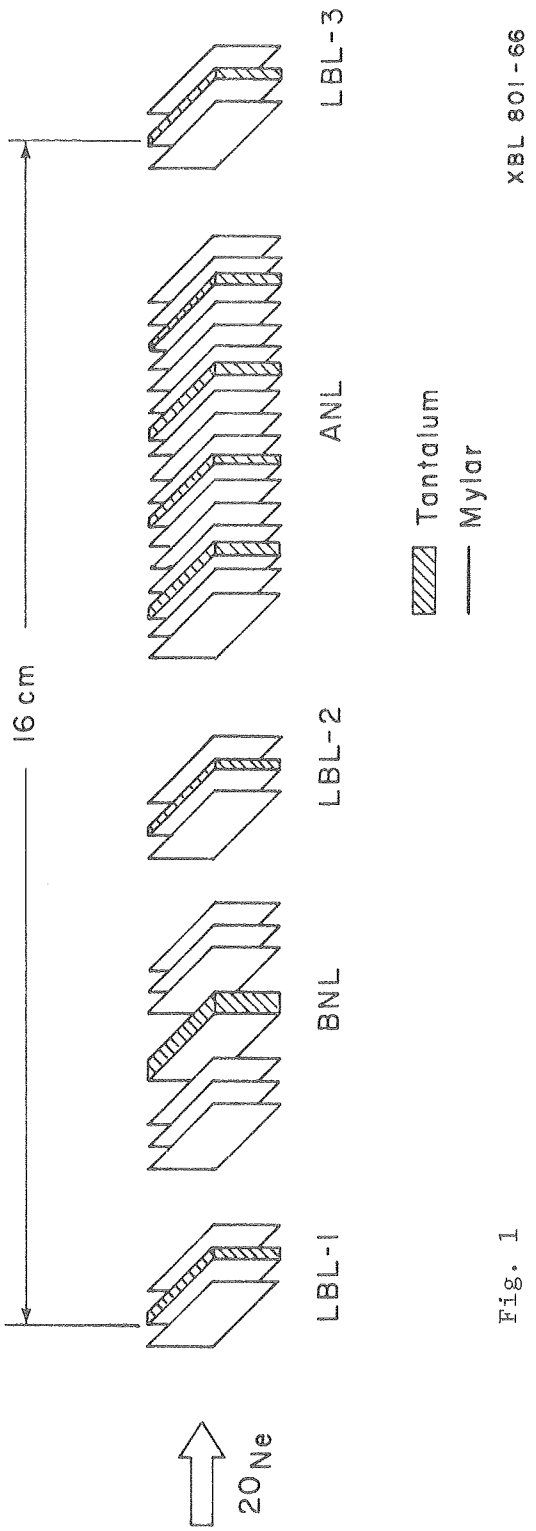

Fig. 1

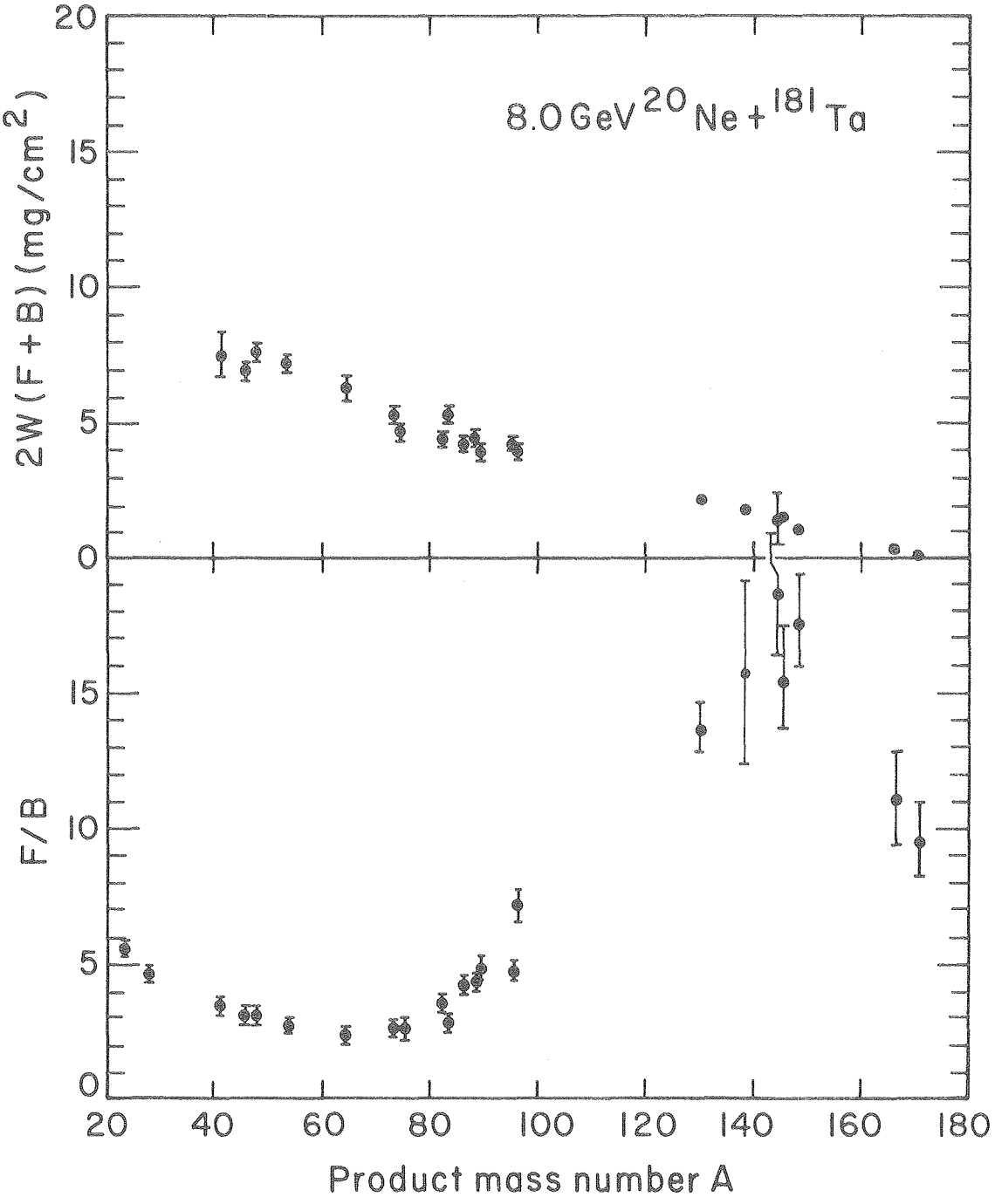

Fig. 2

XBL 801-68

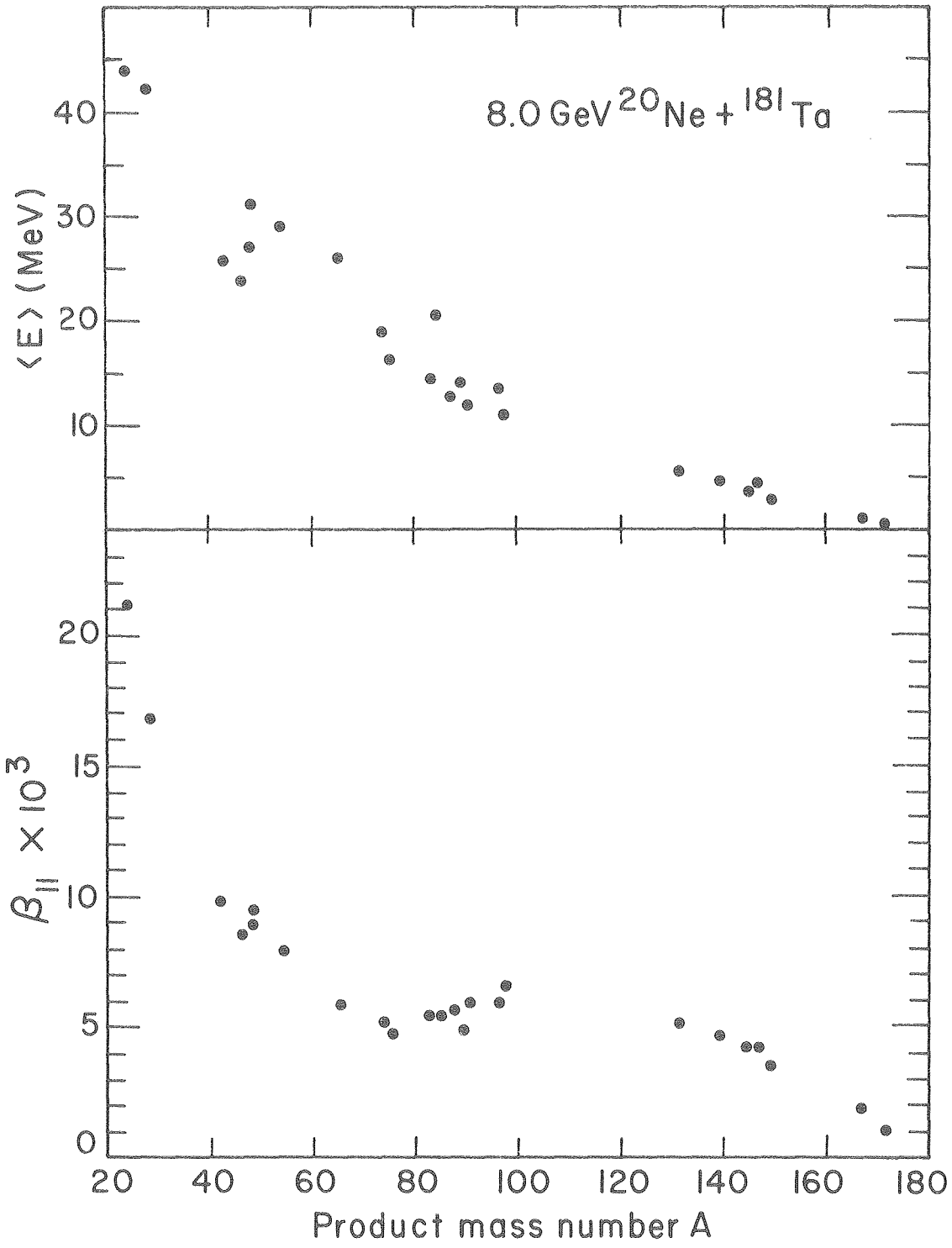

Fig. 3

XBL 801-69

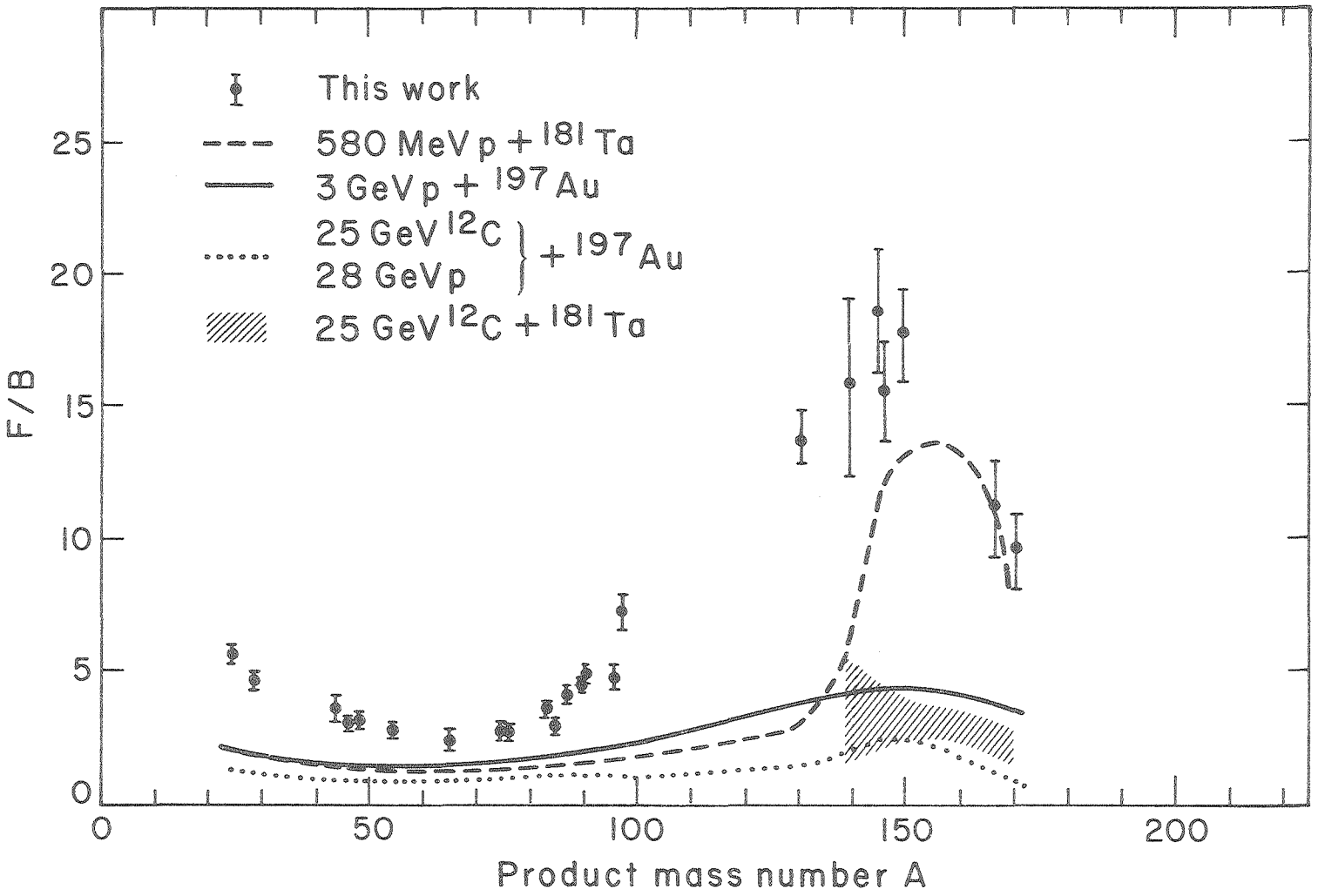

Fig. 4

XBL 801-71

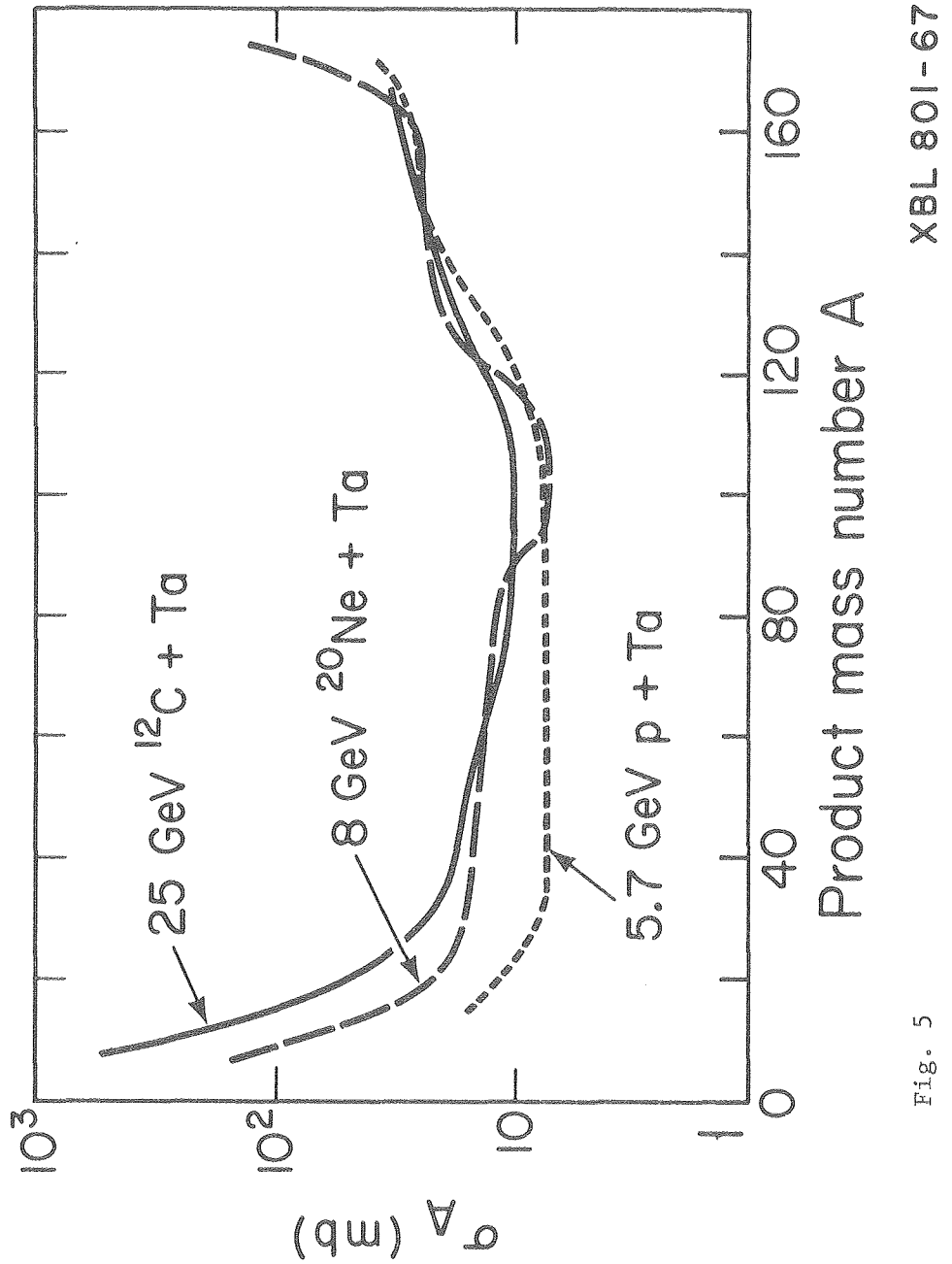

XBL 801-67

Fig. 5

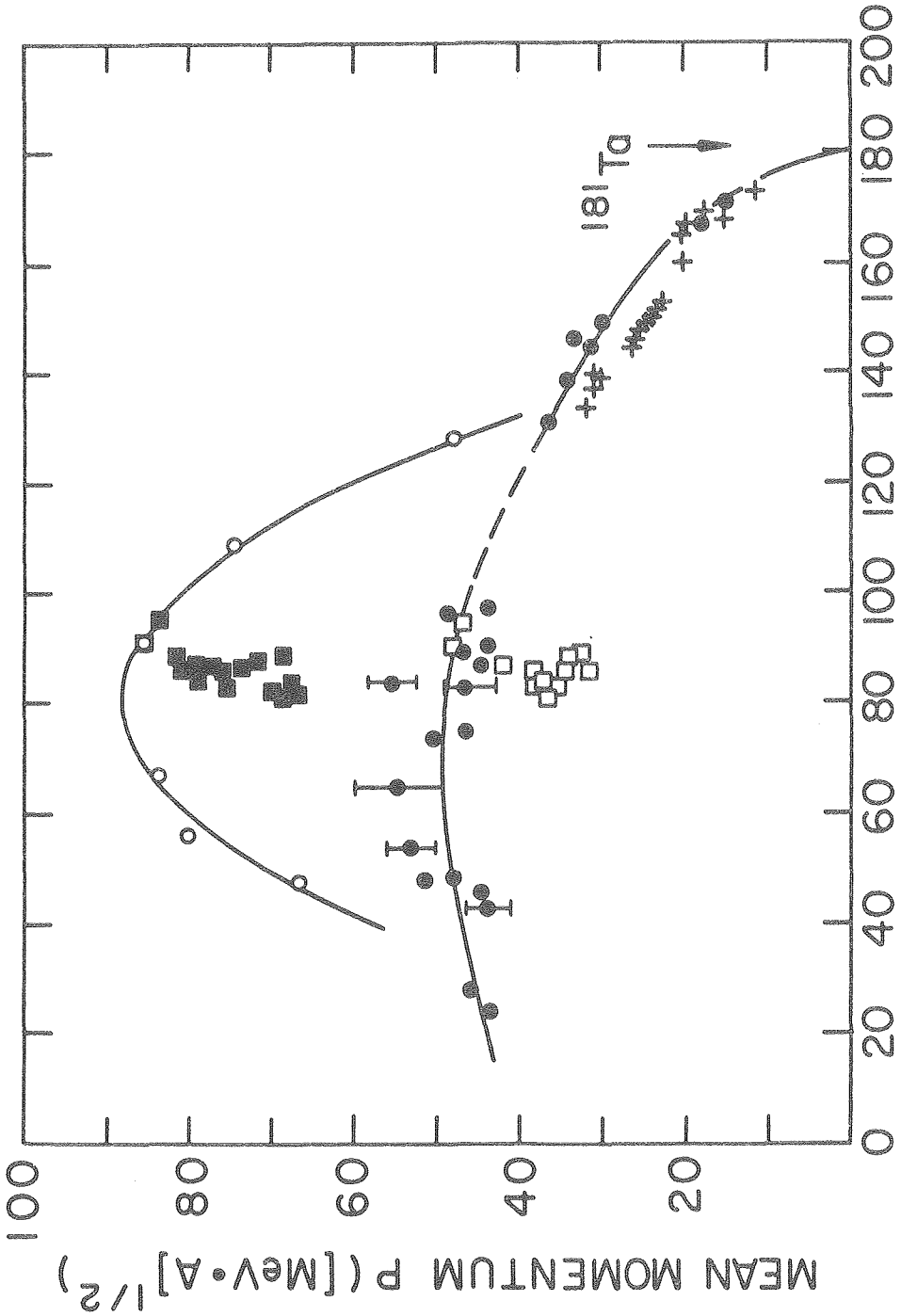

XBL 805-970

Fig. 6

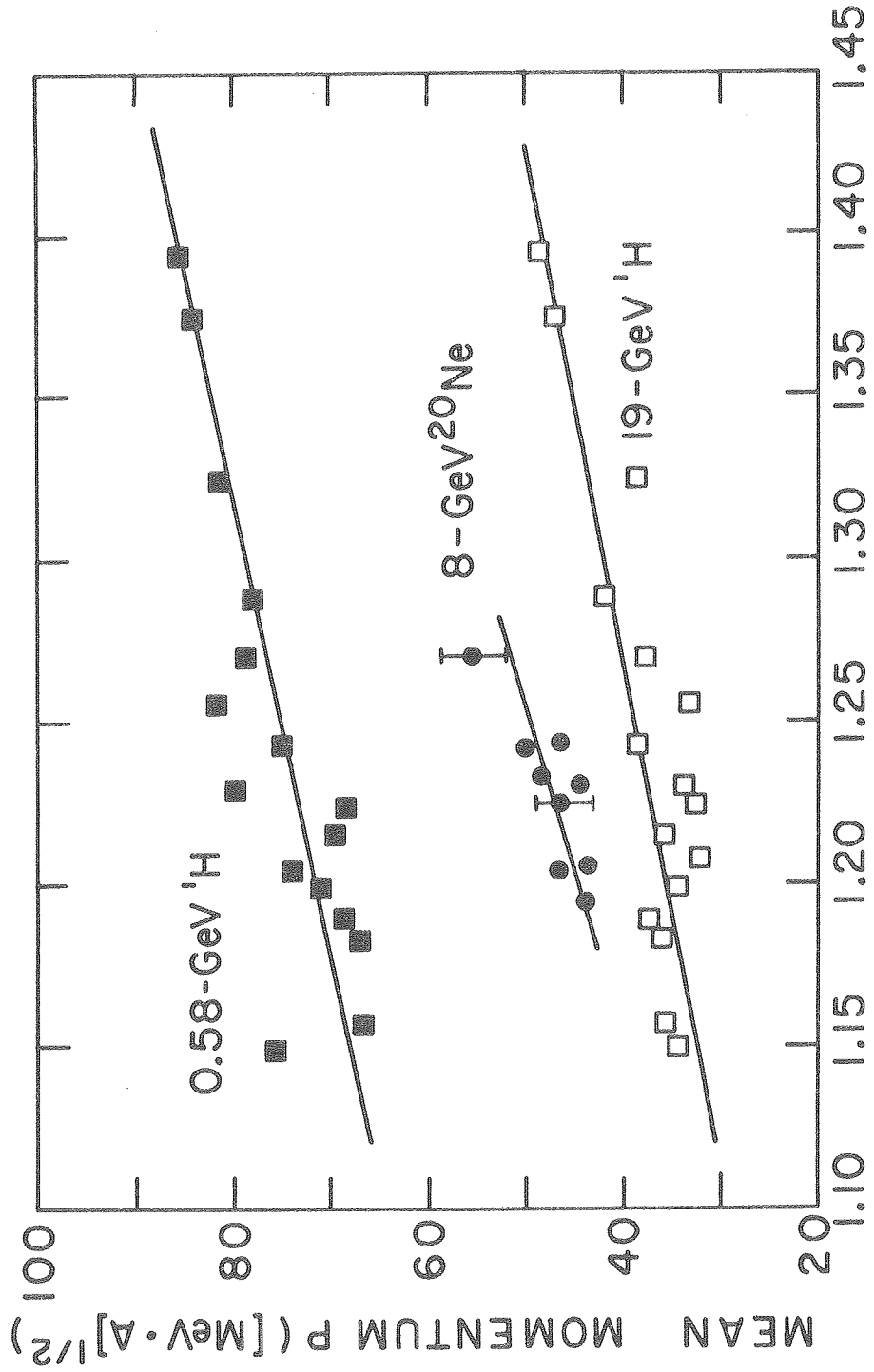

XBL 805-969

Fig. 7